Journal of Metals, Materials and Minerals, Vol.24 No.1 pp.1-6, 2014

Corrosion Study on Low Alloy High Phosphorus Steel

Basanta Kumar JENA[1], Nandita GUPTA[2], Balbir SINGH[3] and Gadadhar SAHOO[3*]

[1]*Dr. B.R. Ambedkar Institute of Technology, Port Blair, A&N Island, India*
[2]*National Institute of Foundry&Forge Technology, Hatia, Ranchi-834003, India*
[3]*R&D Centre for Iron and Steel, SAIL, Doranda, Ranchi-834002, India*

Abstract

The effect of P on corrosion behaviour of low alloy steels exposed for one month cyclic wet/dry salt spray was investigated and compared with low carbon steel. Electrochemical Impedance Spectroscopy (EIS) results revealed that the rust resistance (R_{rust}) increased with the number of salt spray test cycles. The higher phosphorus content steel (G12) exhibited higher rust resistance (R_{rust}) than that of low phosphorus content steels (SCR & G11), while similar corrosion rate was noticed from the Tafel extrapolation study in 3.5% NaCl solution for all the test samples. All steels revealed ferrite pearlite microstructure. The larger ferrite grain of G12 steel containing highest phosphorus content (0.42 wt.% P) is attributed to the effect of phosphorus.

Keywords : Weathering steel, High phosphorus steel, Tafel polarization, Electrochemical impedance spectroscopy, Cyclic salt spray test
DOI : 10.14456/jmmm.2014.1

Introduction

Weathering steels form a compact rust layer during long-term exposure to the atmosphere.[1-6] The compact rust layer gradually becomes denser over time and eventually protects the steel from corrosive environment & thus corrosion is inhibited by the corrosion product. Minor damage to the rust heals itself; therefore maintenance is greatly reduced. Due to such beneficial property, weathering steels have been used for many structural and engineering applications. It is well known that the protective rust layer of weathering steel consists of two layers; a compact, dense, amorphous and adherent inner layer, enriched with some alloying elements such as Cr, Cu, Ni, Mn, and P and a loose crystalline outer layer distributed with cracks and pores.[1,2,7-10] The 1600-year old Delhi Iron Pillar is well known for its remarkable corrosion resistance. This exceptional corrosion resistance has been attributed to the presence of relatively high phosphorus content (0.25 wt.%) in the pillar which plays a major role by facilitating the formation of a protective passive film on the surface.[11,12] As reported by G P Zhou et al.[13], the rust became more homogeneous and compact on increasing P content in cast strips. The P enrichment was observed at the interface between rust layer and substrate, which was believed to be responsible for the improvement of weathering resistance by retarding ingress of aggressive ions and moisture. According to H. Kihira et al.[14], phosphorus forms a thin and protective intermediate phosphatic layer between the outer and inner layer.

Based on these literature findings, the use of higher amount of phosphorus in weathering steels seems to be worthful. The maximum specified value of phosphorus content in CORTEN steel, widely used for structural applications, is 0.15 wt.% with 0.65 wt.% max Ni and 0.55 wt.% max Cu.[15] As Ni is costly, the alternate steel with lower Ni and Cu content and higher phosphorus content will be economically more viable than CORTEN steel. This is the main focus of this paper.

Materials and Experimantal Procedures

Heats of low alloy steels of 25 kg each were made separately utilizing a high frequency induction-melting furnace of 100 kg capacity. Steel scraps of C-Mn rail steel was added to soft iron (0.001 wt.% C) to balance carbon content. The desired P and Cr content of low alloy steels were obtained by adding Fe-P and Fe-Cr mother alloys while Ni lumps and Cu blocks were added to balance Cu and Ni. All mother alloys and metal blocks/lumps were added in furnace. The melts were cast into ingots of cross sectional dimension 10 cm×10 cm. Hot rolling was carried out in two stages. In first stage, the ingots were rolled in five

*Corresponding author E-mail : gadadhar@sail-rdcis.com

passes into 16 mm thickness plate after soaking at 1150°C for 2.5 hours. The finishing temperature was 950°C. In the second stage, once again these plates were soaked for 30 minutes at 1150°C and hot rolled into 5 mm thickness plate in three passes. The finishing temperature was maintained at 800 to 830°C.

Specimens (20mm×15mm×5mm) for metallography examination were grounded successively to 1200 grit water proof SiC paper followed by cloth polishing using alumina suspension up to 0.05 micron. An optical microscope (Olympus GX 71) was used for capturing the photomicrographs after etching the samples with 2% Nital solution (98% alcohol + 2% nitric acid).

Samples of dimension 20 mm × 20 mm × 5 mm were grounded successively to 1200 grit SiC abrasive paper and degreased with acetone for the electrochemical experiments. The polarization experiment was conducted in a standard flat cell (Princeton Applied Research, Ametek, USA) in the potential range –250 mV to +250 mV versus open circuit potential of samples, using a computer controlled potentiostat (Princeton Applied Research, Ametek273A, USA). A saturated silver-silver chloride (SSC) reference electrode with platinum counter electrode was used. The scan rate employed for the polarization studies was 0.25 mVs^{-1}. The corrosion current density (i_{corr}) was evaluated from Tafel plots by the Tafel Extrapolation method as per ASTM Standard G3-89.[16, 17] For the cyclic salt spray test, samples of dimension 70 mm×30 mm×5 mm were grounded down to 60 grit SiC paper, cleaned with acetone and kept for 24 hours in a desiccators. The test samples were placed in the panels at an angle of 45° from vertical. As per ASTM-B117[18], 5 wt.% NaCl solution was used for creating salt fog. The salt spray exposure cycle consisted of 20 minutes wet and 40 minutes dry condition from 10.30 am to 5.30 pm and remaining 17 hours was kept dry at room temperature. The samples were weighed weekly to evaluate % wt. gain.

AC Electrochemical Impedance Spectroscopy (EIS) was performed periodically after second and fourth weeks of cyclic wet–dry salt fog exposure test, using a multichannel potentiostat (Model: VERSASTAT (MC) FRD100). The EIS study was conducted in a freely aerated 3.5% NaCl solution using a standard flat cell supplied by Princeton Applied Research, Ametek, USA. The exposed area of each sample was 1 cm^2. EIS scan was carried out by applying a sinusoidal potential perturbation of 10 mV at the open circuit potentials with frequency sweep from 100 kHz to 100 mHz. All the experimental EIS data were obtained in VERSASTUDIO-2.03 software and modelled using ZSimpwin (version 3.21, Princeton Applied Research, Ametek, USA) software.

Results and Discussion

The chemical compositions of steels obtained using an optical emission spectrometer (OES) are provided in Table 1. Figure 1 shows the typical microstructure of G11 (Figure 1a), SCR (Figure 1b), LC (Figure 1c) and G12 (Figure 1d) along rolling direction obtained using light optical microscope. All photomicrographs consist of ferritic matrix (lighter phase) with pearlite (darker phase) at the grain boundary region. While uniform distribution of pearlite was noticed in G11, SCR and LC, the same is not found in the case of higher phosphorus content (0.42% P) G12.

Furthermore, the ferrite grain size is significantly larger in G12 steel. Other microstructural feature is that the grain size is relatively smaller in the case of LC than that of G11 and SCR. These finding indicates that phosphorus increases grain size of ferrite and the effect is significant with higher phosphorus content. Tafel polarisation was carried out on freshly grounded samples and the behaviour of corresponding Tafel plots of G11, G12, SCR and LC steels in 3.5% NaCl solution is shown in Figure 2. The cathodic branch of all Tafel plots are diffusion controlled. This is expected as NaCl solution is aerated and neutral where the cathodic reaction consists of the oxygen reduction ($O_2 + 2H_2O + 4e \rightarrow 4OH^-$).[19,20] This is also evident from Pourbaix diagram of Fe-H_2O system.[21] Here, diffusion controlled oxygen reduction is the only dominant reaction at ZCP, for which the linear cathodic Tafel region is absent.[19] The i_{corr} and corrosion rate (mpy) obtained from the Tafel polarisation curves of samples under investigation are tabulated in Table 2. The E_{corr} of the samples lies between -500 mV SCE to 600 mV SCE. The corrosion rate of all samples is in good agreement with the literature findings.[22-24] The reported corrosion rate of samples of low alloy, C-Mn, and high phosphorus steel obtained by the Tafel extrapolation method after 1 hour immersion in 3.5% NaCl was in the range of 6 to 10 (mpy), where the alloying elements had no effect on

corrosion rate.[22] In the present study, the corrosion rate of all samples obtained by Tafel Extrapolation method after 45 minutes immersion in 3.5% NaCl is in the range of 9 to 12 mpy (Table 2). Thus, the Tafel polarization study showed that the presence of the alloying elements like Cu: 0.30-0.35, Cr: 0.36-0.37, Ni: 0.20-0.31 and P: 0.15-0.42 has no effect on reducing corrosion rate in 3.5% NaCl although the contents of alloying element is higher than that of the low alloy steel used in the study of Sahoo and Balasubramaniam.[22

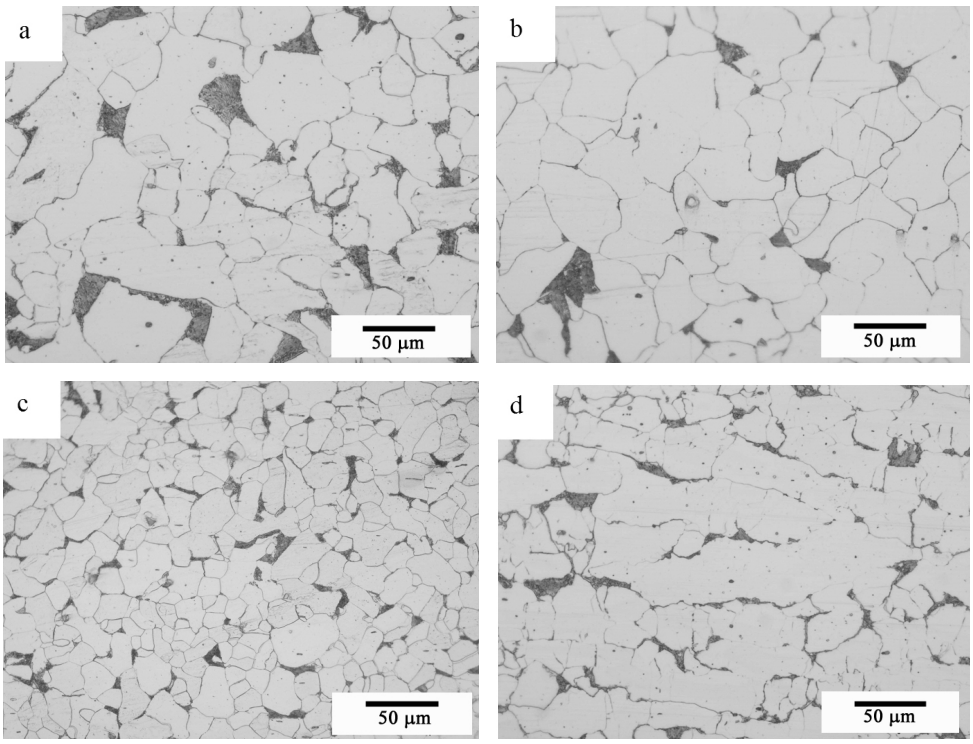

Figure 1. Photomicrograph of hot rolled (a) G11, (b) SCR, (c) LC and (d) G12 along cross section

Table 1. Chemical compositions of the investigated steels, G11, G12, SCR & LC (in wt.%)

Sl no	samples	C	Si	Mn	S	P	B	Cr	Cu	Ni	N	Al
1	G-11	0.085	0.085	0.24	0.009	0.25	0.0022	0.36	0.30	0.20	0.005	0.02
2	G-12	0.085	0.09	0.28	0.007	0.42	0.0022	0.36	0.30	0.20	0.005	0.011
3	SCR	0.09	0.37	0.42	0.01	0.15	-	0.37	0.35	0.31	0.005	0.03
4	LC	0.086	0.11	0.29	0.01	-	-	-	-	-	-	0.03

Table 2. i_{corr} and corrosion rate (mpy) of hot rolled G11, G12, SCR, and LC steel calculated from Tafel plots

Sample	i_{corr} ($\mu A/cm^2$)	Corrosion Rate (mpy)
G-11	21.44	9.5
G-12	26.03	11.93
SCR	22.60	10.36
LC	21.75	9.95

The Nyquist plots obtained in 3.5% NaCl solution after 2nd and 4th week of cyclic wet/dry salt spray test for all the steels are shown in Figure 3&4. The Nyquist plots for all the samples showing double time constants are represented by two semi circles. The corresponding equivalent circuit model used for the impedance data is R_S (Q_{edl} R_{ct}). Here, R_S is the solution resistance between reference electrode and metal surface, Q_{edl}&R_{ct} are the constant phase elements of the electric double layer (EDL) and the charge transfer resistance of the metal/electrolyte interface, respectively. As per equivalent circuit modeling as well as Figure 3 and 4, the value of R_{ct} is highest for the high phosphorus steel (G12) followed by G11 and SCR. However, the trend of R_{ct} value for G11 and SCR has been reversed although in a close range after 4th week of test. This may be due to the effect of higher Si content in SCR. R_{ct} is the lowest for low carbon steel in both the cases as no alloying element is present in this steel.

The results obtained from wet-dry cyclic corrosion test can be compared with the literature where similar types of studies are carried out. A. Nishikata et al.[25] had reported that in a relatively mild environment, the corrosion rate of weathering steel is similar to that of C-Mn steel at the early stage of exposure. However, the corrosion rate was reduced after long term exposure due to the formation of dense and compact rust layer. This behaviour is also evident from the Nyquist plot in Figure 4 after 4 weeks of exposure. R_{ct} has been increased for G11, SCR and G12 dramatically than that shown in Figure 3. The higher phosphorus containing steel G12 has shown more R_{ct} value both after 2 and 4 weeks of exposure. This is attributed to the formation of some phosphatic intermediate layer as observed by Kihira et al.[14]

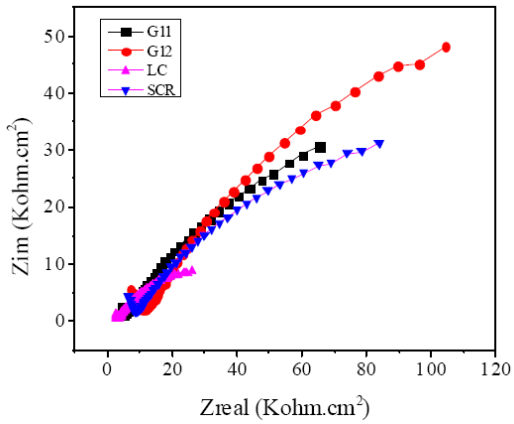

Figure 3. Nyquist plot of as received samples G11,G12, SCR and LC after 2nd week of wet/dry salt spray exposure.

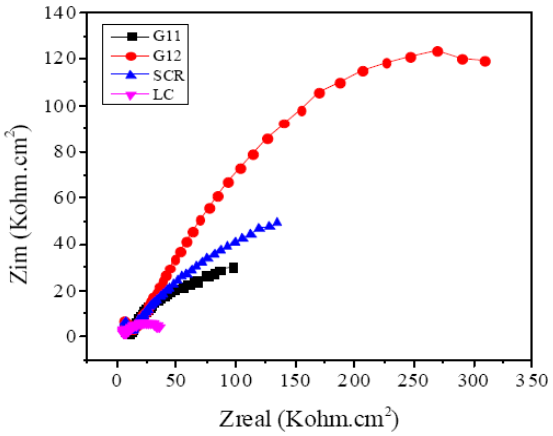

Figure 4. Nyquist plot of as received samples G11,G12, SCR and LC after 4th week of wet/dry salt spray exposure

Conclusions

Tafel polarization study of low alloy high phosphorus and low carbon steel in 3.5% NaCl solution revealed that the alloying elements, e.g. Cr, Cu, Ni and P in the range of 0.36-0.37, 0.30-0.35, 0.20-0.31 and 0.15-0.42.wt.% respectively, have no effect in reducing corrosion rate in immersion condition. The linearity of cathodic region was absent due to diffusion controlled oxygen reduction reaction. However, the beneficial effects of alloying elements, especially phosphorus in reducing metal dissolution was well understood from electrochemical impedance spectroscopy test of samples exposed to cyclic wet-dry salt spray chamber. The charge transfer resitance (R_{ct}) was increased significantly on increasing wet-dry cyclic periods. All steels revealed ferrite pearlite microstructure with higher ferrite grain size in the case of high phosphorus G12 steel.

Acknowledgement

Authors are very much thank full to the management of R&D Centre for Iron and Steel, SAIL, Doranda, Ranchi for providing the necessary support to carry out this work. Authors are also thankful to the corresponding laboratory personnel for their full support and help in conducting experiments.

References

1. Townsend, H.E., Simpson, T.C. and Johnson, G. L. (1994). Structure of rust on weathering steel in rural and industrial environments. *Corrosion*. **50(7)** : 546-554.

2. Stratmann, M. and Streckel, H. (1990). On the atmospheric corrosion of metals which are covered with thin electrolyte layers-II. Experimental results. *Corros. Sci*. **30(6-7)** : 697-714.

3. Zhang, C., Cai, D., Liao, B., Zhao, T. and Fan, Y. (1990). A study on the dual-phase treatment of weathering steel 09CuPCrNi. *Mater. Lett.* **58(9)** : 1524-1529.

4. Hao, L., Zhang, S., Dong, J. and Ke, W. (2012). A study of the evolution of rust on Mo–Cu-bearing fire-resistant steel submitted to simulated atmospheric corrosion. *Corros. Sci.* **54** : 244-250.

5. De la Fuente, D., Díaz, I., Simancas, J., Chico, B. and Morcillo, M. (2011). Long-term atmospheric corrosion of mild steel. *Corros. Sci.* **53(2)** : 604-617.

6. Wang, Z., Liu, J., Wu, L., Han, R. and Sun, Y. (2013). Study of the corrosion behavior of weathering steels in atmospheric environments. *Corros. Sci.* **67** : 1-10.

7. Okada, H., Hosoi, Y. and Naito, H. (1970). Electrochemical reduction of thick rust layers formedon steel surfaces. *Corrosion.* **26** : 429-430.

8. Meybaum, B. R. and Ayllon, E. (1980). Characterization of Atmospheric corrosion products on weathering steels. *Corrosion*. **36(7)** : 345-347.

9. Suzuki, I., Hisamatsu, Y. and Masuko, N. (1980). Nature of Atmospheric rust on iron. *J. Electrochem. Soc.* **127(10)** : 2210-2215.

10. Murata, T. (2000). *Weathering Steel in Uhlig's Corrosion Handbook*. 3rd ed. New York : John Willey & Sons.

11. Balasubramaniam, R. (2000). On the Corrosion Resistance of the Delhi Iron Pillar. *Corros. Sci.* **42(12)** : 2103-2129.

12. Balasubramaniam, R. and Ramesh Kumar, A.V. (2000). Characterization of Delhi iron pillar rust by X-ray diffraction, Fourier infrared spectroscopy and Mössbauer spectroscopy. *Corros. Sci.* **42(12)** : 2085-2101.

13. Zhou, G.P., Liu, Z.Y., Qiu, Y.Q. and Wang, G.D. (2009). The improvement of weathering resistance by increasing P contents in cast strips of low carbon steels. *Materials and Design*. **30(10)** : 4342-4347.

14. Kihira, H., Ito, S. and Murata, T. (1990). The behavior of phosphorous during passivation of weathering steel by protective patina formation. *Corros. Sci.* **31** : 383-388.

15. US-CORTEN STEEL : Catalogue of US Steel (1977).

16. Ijsseling, F.P. (1986). Application of Electro-chemical methods of corrosion rate determination to system involving corrosion product layers. *Br. Corros. J.* **21** : 95-101.

17. Tait, W.S. (1994). *An Introduction to Electro-chemical corrosion testing for practicing engineers and scientists.* Wisconsin : Pair O Docs.

18. ASTM B117-03. (2006). *Standard Practice for Operating Salt Spray (Fog) Apparatus*. West Conshohochen. PA 19428-2959.

19. Flitt, H.J. and Schweinsberg, D.P. (2005). Evaluation of corrosion rate from polarisation curves not exhibiting a Tafel region. *Corros. Sci.* **47(12)** : 3034-3052.

20. Flitt, H.J. and Schweinsberg, D.P. (2005). A guide to polarisation curve interpretation : deconstruction of experimental curves typical of the $Fe/H_2O/H^+/O_2$ corrosion system. *Corros. Sci.* **47(9)** : 2125-2156.

21. Pourbaix, M. (1966). *Atlas of electrochemical equilibria in aqueous solutions*, 1st ed. New York : Pergamon.

22. Sahoo, G. and Balasubramaniam, R. (2008). Corrosion of Phosphoric Irons in Acidic Environments. *J. ASTM Int.* **5(5)** : 1-7.

23. McCafferty, E. (2005). Validation of Corrosion Rates Measured By the Tafel Extrapolation Method. *Corros. Sci.* **47(12)** : 3202-3215.

24. Dexter, S.C. (1979). *Handbook of Oceanographic Engineering Materials*. New York : John Wiley and Sons.

25. Nishikata, A., Yamashita, Y., Katayama, H., Tsuru, T., Usami, A., Tanabe, K. and Mabuchi, H. (1995). An electrochemical impedance study on atmospheric corrosion of steels in a cyclic wet-dry condition. *Corros. Sci.* **37(12)** : 2059-2069.